Transport Studies of the Solid Solutions $X\ SrO+(1-X)Nd_2O_3$: $0.01 \leq X \leq 0.15$

Jun Ho Jang, Kwang Sun Ryu, Don Kim†, Sung Han Lee, Keu Hong Kim, and Chul Hyun Yo

Department of Chemistry, Yonsei University, Seoul 120-749
†General Education Department, Pusan National Institute of Technology, Pusan 608-080
Received November 10, 1992

SrO-doped Nd_2O_3 systems (SDN) containing 1, 5, 10, and 15 mol% SrO were found to be solid solutions by X-ray diffraction (XRD) analysis. The lattice parameters(a) were obtained by the Nelson-Riley method, and the values increased with increasing dopant content. Thermal analysis showed that no phase transition occurred in the temperature range covered in this experiment. The electrical conductivity increases with temperature (450-1150℃), but breaks appear in the conductivity curve, dividing it into two temperature regions. At the high temperatures of 750-840 to 1100℃, the activation energy (E_a) and oxygen pressure dependence of conductivity are found experimentally to be average 1.44 eV and $1/n=1/5.3$, and the possible defects and charge carriers are suggested to be metal vacancies and electron holes, respectively. At the lower temperatures of 450 to 750-840℃, the E_a and $1/n$ values obtained are average 0.51 eV and $1/n=1/7.3$ to 1/8.3, respectively. At the lower temperature, the SDN system may contain a mixed conduction involving ionic conductivity due to diffusion of oxygen ion.

Introduction

Most of nonstoichiometric phases are found in the transition-metal, rare-earth, and actinide oxides. Among the rare-earth metal oxides, the dioxides generally exhibit the fluorite structure. The crystal structures of the sesquioxides have been termed the A-, B-, C-, X- and H-type structures. The A-type structure has a hexagonal unit cell and has a sevenfold coordination about the metal ions. The H-type structure is hexagonal similar to that of the A-type. Pratap *et al.*[1] measured the electrical conductivity and dielectric constant of C-type Nd_2O_3 at 400-1100 K and found that a phase transition occurred at about 850 K which was observed both in $\log \sigma$ *vs.* $1/T$ as well as ε' *vs.* T curves. From the thermoelectric power measurements, electron hole conductivity was suggested at higher temperature. On the other hand, Dar and Lal[2] measured the electrical conductivity and dielectric constant of A-type hexagonal Nd_2O_3 pellets at 300-1200 K. They found that the conductivity is described in terms of impurity nature and space-charge polarization of thermally generated charge carrier exists above 500 K. An impurity nature was also found by Volkenkova *et al.*[3] who measured the electrical conductivity of Nd_2O_3 at 500-1000℃ and P_{O_2} of 10^{-4} to 1 atm. Below 700℃ at $P_{O_2}<10^{-2}$ atm, and above 800℃ at the same P_{O_2}, the conductivity is proportional to $P_{O_2}^{1/6}$ and $P_{O_2}^{1/4}$, respectively.

The aim of this work is to proceed with studies of the lower valence cation-doped Nd_2O_3 system. In this paper, likely defect structures, conduction mechanisms, and charge carriers for the SrO-doped Nd_2O_3 (SDN) system have been determined by interpretation and analysis of X-ray result and measurement of electrical conductivity.

Experimental

Sample preparation. The starting powders used were $SrCO_3$ (extra pure, Junsei Chem. Co.) and Nd_2O_3 (99.99%, Aldrich Chem. Co.). They were precalcinated at 800℃ for 24 h to eliminate adsorbed gases, H_2O, NH_3, CO_2, etc., weighed to give Nd_2O_3 containing 1, 5, 10, and 15 mol% SrO, ball-milled for several hours in ethanol, and fully dried at 230℃. These samples were made into pellets under a pressure of 98.06 Mpa under vacuum at room temperature. The pellets were sintered at 1250℃ for 72 h, annealed at 1150℃ for 48 h, and then quenched to room temperature. The samples were analyzed by the XRD technique to determine whether each sintered SDN sample was a complete solid solution. The samples analyzed by X-ray diffraction angle analysis (Philips, PW 1710, CuKα) were polished with abrasive paper until the voids of the interface region of the specimen were fully eliminated, and then made into rectangular form with dimensions of $1.2\times0.7\times0.2$ cm^3. Four holes were drilled in a row on one face for a 4-probe contact.

Conductivity measurements. The electrical conductivity was measured at 500 to 1100℃ under 2×10^{-5} to 2×10^{-1} atm oxygen pressure. The calculations of the conductivities were carried out by the Valdes techniques[4]; $\sigma=(1/2\pi S)I/V$ where S, I and V are the distances between each probe, the current and potential through the sample, respectively. The current through the sample was maintained between 10^{-9} and 10^{-4} A, and the potential across the inner two probes was maintained between 0.1 and 1.5 V. The current through the sample was measured by a multirange electrometer (Keithley Instruments 610 C, Cleveland, OH) and the potential difference was measured by a potentiometer (Leeds and Northrup 7555 type K-5 North Wales, PA).

Results and Discussion

XRD analysis

The crystal structure, the formation of solid solution and the accurate lattice parameter(a) for each sintered SDN sample were undertaken by the following procedures. X-ray diffraction peaks for the SDN samples were obtained by the

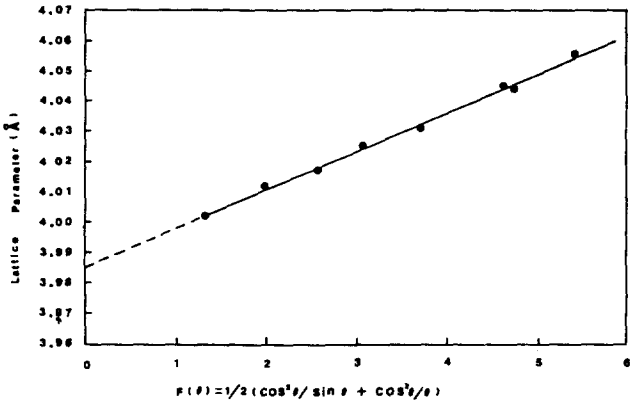

Figure 1. Plot of lattice parameter *vs.* Nelson-Riley function for a 5 mol% SDN system.

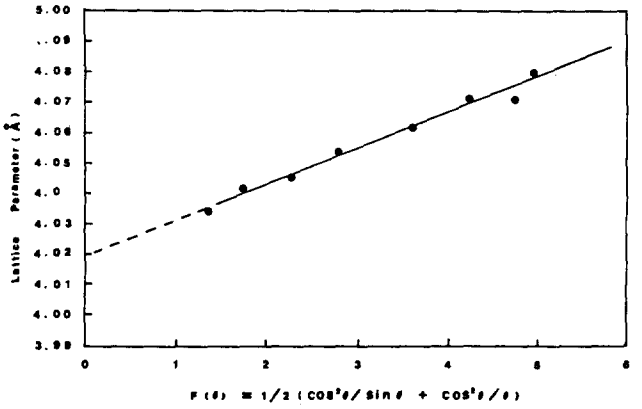

Figure 2. Plot of lattice parameter *vs.* Nelson-Riley function for a 15 mol% SDN system.

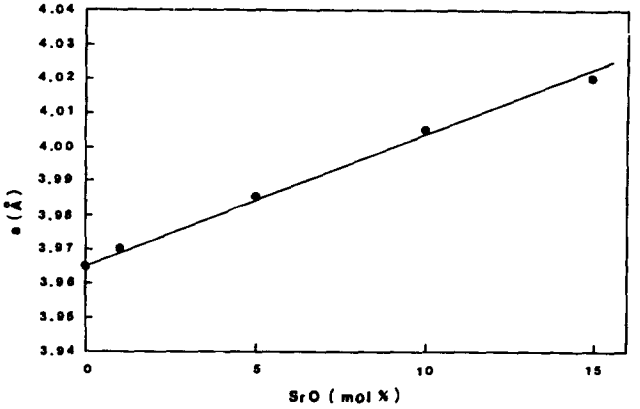

Figure 3. Lattice parameter (a) obtained from the plot of a *vs.* Nelson-Riley function *vs.* SrO mol% for the SDN system.

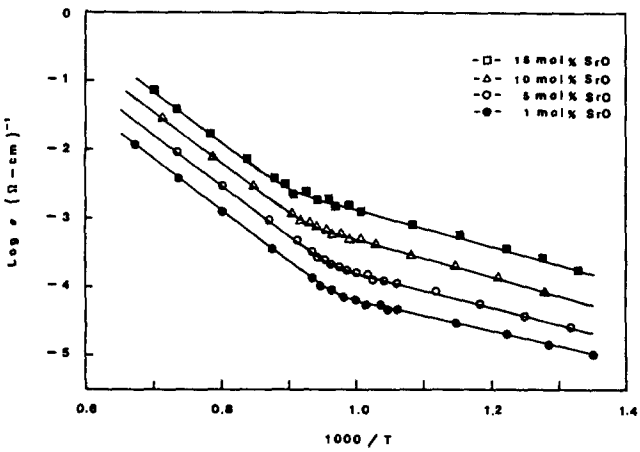

Figure 4. Log conductivity *vs.* $1000/T$ for the 1, 5, 10 and 15 mol% SDN systems under P_{O_2} of 2×10^{-1} atm.

powder method and an exact a value for each sample was made using Nelson-Riley function[5]; each a value was obtained from the *y*-axis intercept of a plot of a value against the $F(\theta)=(\cos^2\theta/\sin\theta+\cos^2\theta/\theta)/2$. Strickler and carlson[6] have reported that the lattice parameters show linearity only in the region where complete solid solutions are established in the plots of lattice parameters *vs.* dopant mol% for various cation-doped solid solutions. Thus, the formation of solid solutions can be interpreted from the linearity of the data points for each sample in the plot of lattice parameters *vs.* dopant mol%.

The lattice parameter of pure Nd_2O_5, obtained from the *y*-axis intercept in a plot of a value against the Nelson-Riley function, was an a value of 3.965 Å, which agrees with the value listed in ASTM ($a=3.960$ Å). The fittings of the lattice parameters for 5 and 10 mol% SDN sample are shown in Figures 1 and 2. Figure 3 shows the lattice parameters obtained from those plots as a function of SrO mol%. As shown in Figure 3, the plot of the lattice parameter *vs.* SrO mol% shows a good linearity up to 15 mol% SDN. Lopato *et al.*[7] reported in their phase-diagram study that in the system Nd_2O_3-SrO of hexagonal structure, a solid solution region was found in the system centered on about 33 mol% SrO. Applying Vegard's law to the present samples formed by random substitution or distribution of ions, it assumes implicitly that the changes in lattice parameters with composition are governed by the relative sizes of the atoms or ions which are active in the solid-solution process in a simple substitutional mechansim. The increase in lattice parameter with increasing SrO mol% shown in Figure 3 can be explained by the fact that the ionic radius of Sr^{2+} (1.120 Å) is larger than that of Nd^{3+} (0.995 Å), or, in other words, that the lattice parameter increases because of the increasing addition of dopant with larger ionic radius. According to Vegard's law, the lattice parameters of our samples with doping impurities shoud change linearly with composition in the solid solution region. From the data in Figure 3, it is concluded that our sampels are all solid solutions.

Electrical conductivity

In SrO-doped Nd_2O_3 solid solution, possible defect structures which can be predicted in nonstoichiometric compositions are classified into excess metal (oxygen deficiency) and excess oxygen (metal deficiency). The predominant defects in case of oxygen deficiency are oxygen vacancies or interstitial metal ions and in case of metal deficiency are metal vacancies or interstitial oxygen atoms.

Figure 4 shows a plot of log σ *vs.* $1/T$ for the 1, 5, 10 and 15 mol% SDN systems and a break of log σ near 750-840℃. From the slope in a plot of log conductivity against the reciprocal of the absolute temperature, the activation energy

Table 1. Activation Energies of the Various SDN Systems at Constant P_{O_2} of 2×10^{-1} atm in the High- and Low-Temperature Regions

SrO mol%	E_a (eV)	
	High temp. (750~840-1150℃)	Low temp. (450~750-840℃)
1	1.40	0.45
5	1.49	0.50
10	1.44	0.55
15	1.43	0.55

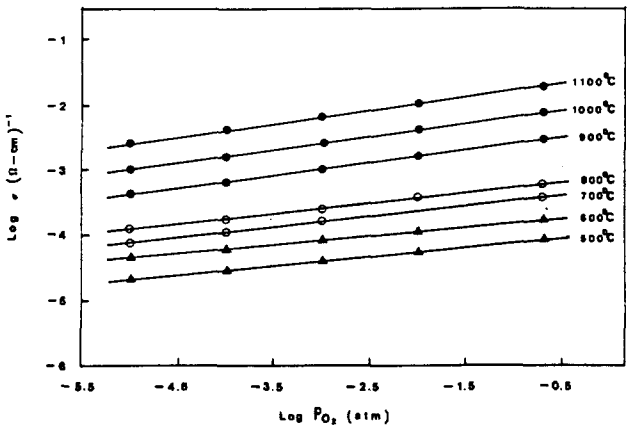

Figure 5. Electrical conductivity as a function of P_{O_2} for a 10 mol% SDN system at various temperatures.

(E_a) in the equation $\sigma=\sigma_o \exp(-E_a/RT)$ for each sample can be calculated. The E_a values obtained from the slopes of plots of log σ *vs.* $1/T$ for various SDN systems fall into two regions of high and low temperatures, and these calculated values are also listed in Table 1.

Figure 5 shows the dependence of electrical conductivity on oxygen partial pressure for the 10 mol% SDN sample as a plot of log σ against log P_{O_2} at various temperatures. As can be seen in this figure, it is apparent that the SDN system has a *p*-type character, shown by the increase of electrical conductivity with increasing temperature and oxygen partial pressure. The electrical conductivity dependences on oxygen partial pressures for the other mol% SDN systems show the same trend as for 10 mol% system. The n values in $\sigma \propto P_{O_2}^{1/n}$ from the slopes in Figure 5 obtained at the various temperatures show a difference in the two temperature regions of 500 to 800℃ and 900 to 1100℃. These results are listed in Table 2.

In this SDN system, the E_a and $1/n$ values are different in higher and lower temperature ranges. The suggested conduction mechanism for the two temperature regions are different. Also, in this system there may be two different defect formation due to oxygen diffusion, because the electrical conductivity increases with increasing oxygen partial pressure. We first assume that the possible defects in this system are metal vacancies at higher temperatures and oxygen interstitials at lower temperatures for the electronic *p*-type semiconductor.

Electrical conduction mechanism

Table 2. Temperature Dependence of the $1/n$ Values for Each of the SDN Systems

Temp. (℃)	$1/n$ values			
	1 mol%	5 mol%	10 mol%	15 mol%
500	1/8.3	1/8.3	1/8.3	1/8.3
600	1/8.3	1/8.3	1/8.4	1/8.5
700	1/7.3	1/7.3	1/7.3	1/7.4
800	1/7.3	1/7.3	1/7.3	1/7.4
900	1/5.4	1/5.4	1/5.3	1/5.2
1000	1/5.3	1/5.3	1/5.3	1/5.2
1100	1/5.2	1/5.3	1/5.3	1/5.3

Possible defect formation at higher temperature. The $1/n$ values for 1, 5, 10 and 15 mol% SrO-doped Nd_2O_3 systems are 1/5.2-1/5.4 in the higher temperature region and 1/7.3-1/8.3 in the lower temperature region, as shown in Table 2. The activation energies (E_a) obtained at temperatures above 450℃ are 0.45-0.55 eV (Table 1). These E_a values imply that the donors are already saturated in the donor level. On the other hand, the activation energies obtained at temperatures above about 800℃ are 1.40-1.49 eV (Table 1). These E_a values are very larger than the values in the lower temperature region and are somewhat larger than the value reported by Partap *et al.*[1], who observed the energy band gap of 1.91 eV for pure Nd_2O_3 in both log σ *vs.* $10^3/T$ and ε' *vs.* T curves. This larger value is explained by the fact that energy for the formation of electronic defects is needed at higher temperatures.

As shown in Figure 4, the electrical condcutivities increase with increasing SrO mol%. This results indicated that the electron hole density may increase with increasing mol% of SrO. The increase of electron hole density is due to Sr ions acting as electron hole donors according to the principle of controlled valency. This increase in electron hole density should be represented by the doping of strontium.

$$Sr_{Sr} + O_o^x \rightleftarrows Sr'_{Nd} + O_o^x + 1/2\ V_o^{\cdot\cdot} \quad (1)$$

The effectively doubly ionized oxygen vacancies ($V_o^{\cdot\cdot}$) formed by Sr doping [Eq. (1)] react with oxygen molecules, and then electron holes ($\dot{h}$) are created as shown by the following equilibrium:

$$V_o^{\cdot\cdot} + 1/2\ O_2(g) \rightleftarrows O_o^x + 2\dot{h} \quad (2)$$

If the equilibria (1) and (2) exist in SDN system, their sum can be represneted as

$$Sr_{Sr} + 1/2\ O_2(g) + 1/2\ V_o^{\cdot\cdot} \rightleftarrows Sr'_{Nd} + O_o^x + 2\dot{h} \quad (3)$$

where Sr'_{Nd} is effectively singly ionized strontium doped into a Nd ion site. Eq. (3) should contribute to the electrical conduction in this temperature region, since the conductivity increases with increasing SrO mol%.

On the other hand, the predominat defects for pure Nd_2O_3 are triply ionized metal vacancies. The disorder reaction for the formation of metal vacancies can be written as

$$3/4\ O_2(g) \rightleftarrows 3/2\ O_o^x + V'''_{Nd} + 3\dot{h} \quad (4)$$

where V'''_{Nd} is effectively triply ionized metal vacancy. From equilibria (3) and (4), the electrical conductivity dependence

on P_{O_2} can be derived for the SDN samples. The sum of Eqs. (3) and (4) is represented as follows:

$$Sr_{Sr} + 5/4\ O_2(g) + 1/2\ V_o^{\cdot\cdot} \rightleftarrows Sr'_{Nd} + 5/2\ O_o^x + V'''_{Nd} + 5\ h \quad (5)$$

In equilibria (3) and (4), the equlibrium constants are $K_3 = (Sr'_{Nd})P^2(V_o)^{-1/2} \cdot P_{O_2}^{-1/2}$ and $K_4 = (V'''_{Nd})P^3 \cdot P_{O_2}^{-3/4}$, respectively where P is electron hole concentration. In equilibrium (5), the equilibrium constant K_5 is $K_3 \cdot K_4 = (Sr'_{Nd})(V'''_{Nd})P^5(V_o^{\cdot\cdot})^{-1/2} \cdot P_{O_2}^{-5/4}$. The electroneutrality condition is $2(Sr'_{Nd}) + 3(V'''_{Nd}) = (h)$. Assuming $(Sr'_{Nd}) = 2(V_o^{\cdot\cdot})$, $(V'''_{Nd}) = 1/3(h)$, and $(Sr'_{Nd}) = 1/2\ (h)$ in equilibria (1), (4) and (3), K_5 can be written as follows:

$$K_5 = 1/3\ P^{13/2} \cdot P_{O_2}^{-5/4} \quad (6)$$

Since the electrical conductivity (σ) is proportional to electron hole concentration (P) on the SDN system, the electrical conductivity dependence on P_{O_2} should be represented as follows:

$$\sigma \propto P = (9K_5^2)^{1/13} \cdot P_{O_2}^{1/5.2} \quad (7)$$

or

$$\sigma = K' \cdot P_{O_2}^{1/5.2} \quad (8)$$

whrer K' is $k(9K_5^2)^{1/13}$.

As can be seen in Table 2, P_{O_2} dependence of conductivity in the higher temperature region is $1/n = 1/5.2$-$1/5.4$. The predicted value from the equilibria (1)-(5), is consistent with the experimentally observed value of $\sigma \propto P_{O_2}^{1/5.2}$. We can conclude that the possible defects at higher temperature region are metal vecancy and effectively a negatively charged strontium substituted on a Nd ion site, and the electrical conduction is carried by the electron hole created by the two possible defects described in the equibria (1)-(5).

Possible defect formation at lower temperature. The activation energies obtained at temperatures below about 800℃ are 0.45-0.55 eV, as shown in Table 1. Thases E_a values are smaller than the 0.96 eV reported for pure Nd_2O_3[1]. This smaller activation energy is explained on the basis that the defect formation is facilitated by the addition of SrO impurity and the carriers may be saturated in the donor sites. On the other hand, in this temperature region, the P_{O_2} dependence of electrical conductivity is 1/8.3-1/7.3, as shown in Table 2. Because of this P_{O_2} dependence, the possibility of a mixed conduction should be suggested. As was mentioned already, in case of oxygen intersitials being the predominant defect at low temperatures, the oxygen partial pressure dependence of the conductivity can be dervied as $\sigma \propto P_{O_2}^{1/6}$, assuming that the doubly ionized oxygen interstitials predominate in this temperature region. Our data in Table 2 are not fitted to this value, $1/n = 1/6$, implying that the conductivity is not carried by only electron hole.

Berard and Wilder[8] reported on the diffusion of cations and anions in lanthanide oxide that the activation energy values for cations are larger than those for anions, and the movement of oxygen ions through the ⟨111⟩ open pathway is promoted. Eyring and Holmberg[9] also reported on the diffusion of lanthanide oxides that the movement of oxygen is possible even at the low temperature of 400℃, but no mobile cations are observed even at the high temperature of 1200℃. Based on these reports, we suggest that SrO-doped Nd_2O_3 may include ionic conduction owing to the diffusion of oxygen atoms through ⟨111⟩ open pathways even at low temperatures.

The present SDN systems, similarly, can also be expected to have many oxygen vacancies, and thus the diffusion of oxygen is promoted. The ionic conductivity is increased by this diffusion of oxygen atoms. As a result of ionic diffusion, an increase in ionic conductivity may be expected, and the conductivity is unaffected by the oxygen partial pressure in the lower temperature region.

We can draw the following conclusions for lower temperatures. Although the Nd_2O_3 is in fact a pure electron hole semiconductor, the ionic contribution is assumed to result from the electron holes produced by the predominant defect (V'''_{Nd}) of the Nd_2O_3 as determined by Sr ion doping which produces an oxygen vacancy. This oxygen vacancy may act as a diffusion site contributing to an ionic conductivity, producting electron holes. The experimentally observed $\sigma \propto P_{O_2}^{1/7.3} \sim P_{O_2}^{1/8.3}$ can not be obtained regardless of whether V'''_{Nd} or $V_o^{\cdot\cdot}$ predominates or both defects coexist in the SDN sample.

If the electron hole conductivity is coupled with an ionic conductivity which is independent of the P_{O_2}, the oxygen pressure dependence on electrical conductivity should decrease. In this work, since $1/n = 1/5.2$ in $\sigma \propto P_{O_2}^{1/n}$ in the higher temperature region arrives at $1/n = 1/7.3 \sim 1/8.3$ in the lower temperature region, the present SDN systems may include an ionic conductivity.

Acknowledgement. The present works were supported by the Basic Science Research Institute Program, Ministry of Education of Korea, 1991.

References

1. V. Pratap, B. K. Verma, and H. B. Lal, *Proc. Natl. Acad. Sci., India, Sect.*, **A48**, 20 (1978).
2. N. Dar and H. B. Lal, *Pramana*, **7**, 245 (1976).
3. Z. S. Volkenkova and V. N. Chebotin, *Izv. Akad. Nauk SSSR, Neorg. Mater*, **10**, 1275 (1974).
4. L. B. Valdes, *Proc. IRE*, **42**, 420 (1954).
5. J. B. Nelson and D. P. Riley, "An Experimental Investigation of Extrapolation Methods in the Derivation of Accurate Unit-Cell Dimensions of Crystals", *Proc. Phys. Soc. London*, **57**, 160 (1945).
6. D. W. Strickler and W. G. Carlson, *J. Am. Ceram. Soc.*, **47**, 122 (1964).
7. L. M. Lopato, L. I. Lugin, and A. V. Shevchenko, *Soc. Prog. Chem.*, **39**, 27 (1973).
8. M. F. Berard and D. R. Wilder, "Cation Self-Diffusion in Polycrystalline Y_2O_3 and Er_2O_3", *J. Am. Ceram. Soc.*, **52**, 85 (1969).
9. L. Eyring and B. Holmberg, Nonstoichiometric Compounds: p. 46, Am. Chem. Soc. Washington, D. C., 1963.